Pilot studies on optimizing land use, building density and solar electricity generation in dense urban settings

Zhongming Shi[1 2], Shanshan Hsieh[1 2 3], Bhargava Krishna Sreepathi[1 2], Jimeno A. Fonseca[1 2], François Maréchal[1 3], Arno Schlueter[1 2]

[1]Future Cities Laboratory, Singapore-ETH Centre, Singapore [2]Architecture and Building Systems, ETH Zurich, Zurich, Switzerland [3]Industrial Process and Energy Systems Engineering Group, Ecole Polytechnique Federale de Lausanne, Lausanne, Switzerland
E-mail: shi@arch.ethz.ch, hsieh@arch.ethz.ch, sreepathi@arch.ethz.ch, francois.marechal@epfl.ch, schlueter@arch.ethz.ch

Abstract. *Previous studies have identified links between the urban form and the performance of urban energy systems. Land use and density are two important aspects of urban planning and design. This paper studies the relationship between these aspects and the performance of an urban energy system. For this, the study compares different metrics of land use, density, and energy performance. These metrics are floor area ratio, density gradient, land use ratio, renewable energy share, and the peak electricity import from the city grid. The approach is based on the multi-objective optimization of the urban form. The results offer what-if scenarios on how land-use and density can either maximize the performance of an urban energy system.*

Keywords: Military engineering, fortification, urban bastioned system, poliorcetics, city and territory.

Introduction

Cities consume about three-quarters of the global primary energy (UN-Habitat, 2012). Compared to that of the beginning of the Twenty-first Century, urban areas are expected to triple by 2030 (Seto et al., 2012). The future performance of urban energy systems could be substantially influenced by how urban areas are planned, designed, and built (IEA ECBCS Annex51 - Subtask B, 2012). On the other hand, energy systems could enable new possibilities to shape the form and location of buildings. For example, a district cooling system can free up the building rooftops for more architectural design options, like an infinity pool or a sky garden. Besides, it allows more space to install photovoltaic panels (PV). The urban form of a city, described by its land use and density, could influence the energy performance of a district (Hsieh et al., 2017). This paper focuses on the interdependencies between urban form and PV.

Density (floor area ratio) and land use are the two main controlling parameters in the master plan of most cities in the world. In particular, we assume that density is not homogeneously distributed, but rather may correspond to the sun path and the angle of solar radiation. Such heterogeneous urban density distribution exists for other reasons as well. For example, the density of an area immediately next to a transit station is higher for more accessibility and higher real estate values (Cervero and Guerra, 2011). Acknowledging such a transit-oriented urban typology with specific heterogeneous density distribution exists, we intend to explore if any of its design metrics can have a substantial influence on the performance of the electricity generation from PV panels.

As an example, we place this study in the context of Singapore. The annual irradiation

http://dx.doi.org/10.4995/ISUF2017.2017.5636

in Singapore is 1636 kWh /m2 (Luther and Reindl, 2014), with little seasonal variation. However, the share of diffuse radiation is around 55%, and the daily variability is high due to the frequently changing cloud coverage (Luther and Reindl, 2014). Due to the space limitation, the PV modules are mostly installed on building rooftops or facades. Moreover, as for the transit-oriented urban typology, the Authority of Singapore allows additional built area if the project falls into a certain radius from the transit stations (Urban Redevelopment Authority, 2017).

The Methodology section describes the design of the experiment, including the configuration of the parametric computational model, the optimization setup, and the sorting method of the results. The Results and Discussion presents an application of the method to an Area in Singapore. The Conclusion section concludes with the suggestions on urban design concerning land use and density for high-performance PV electricity generation in Singapore. This section also includes a discussion on the shortcomings of this study and the potential future work.

Methodology

In this work, we chose two metrics regarding energy performance. One was the peak electricity power imported from the grid (PDG) of the entire district, which is the highest surplus between electricity consumption and PV electricity generation over the simulated period. This value can be used to design the operation limits of the distribution grid to the district. The other one was the renewable energy share (%RES), namely the fraction of PV electricity (PVE) supply to the total electricity consumption. To study how urban density and land use affect the energy performance, we adopted the method of simulation-based urban form generation and optimization. The model has three parts, namely, a parametric model of urban form generation, energy simulation, and an optimization engine.

Figure 1 illustrates the workflow of our methodology. We built the parametric model on the platform of Grasshopper at Rhinoceros 3D. We used EnergyPlus (EnergyPlus Energy

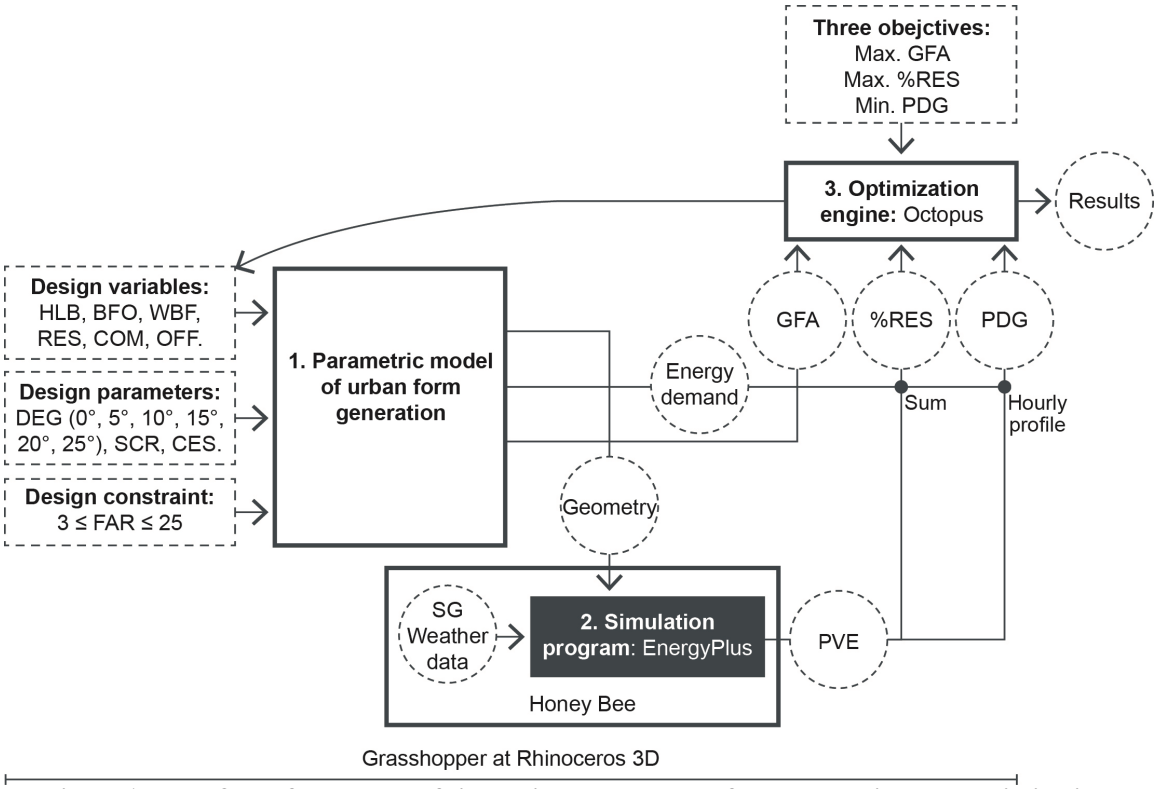

Figure 1. Workflow of the model of simulation-based urban form generation and optimization

Simulation Software, 2017) to simulate the PV electricity generation. EnergyPlus and Grasshopper were connected through the components of HoneyBee. We used the Grasshopper plugin Octopus for optimization.

The metrics fundamental to develop the parametric model are defined in Table 1 and Figure 2. The metrics related to the density include gross floor area (GFA), floor area ratio (FAR), site coverage ratio (SCR), density gradient (DEG), the height of the lowest building per(HLB) and cell size (CES). Land use ratio (LUR) controls the land use. As per the Singapore Master Plan, the most common land use includes residential, commercial, office and industrial. In this work, we excluded industrial land use as it is less likely to appear in a transit-oriented development in the high-density context of Singapore. In addition, we took the building façade orientation (BFO) and the space in between buildings (DBB) into consideration, as they are important factors for solar analysis (Sanaieian et al., 2014).

Figure 2 presents an example of the parametric model. We adopted the most common regular grid street pattern, found through a morphological survey of cells in the six strategic mixed-use centers of Singapore. For each homogeneous individual cell, we used the most predominant podium building pattern with an SCR of 0.45, as 42% of the total 602 cells surveyed have a podium pattern, and the mean SCR of these cells is around 0.45. The CES was also defined using the equivalents in the case studies, which was a size of 100 meters by 100 meters. With the transit station as the center of the district, all the cells fell into a radius of 400 meters, which was defined by the average walking distance of Singaporeans (Olszewski and Wibowo, 2005). There were six design variables involved defining the parametric model of urban form generation. They were HLB (33-165m, with 3 meters' increment), WBF (50-90m, with

Table 1. Metrics constituting the parametric model

Metrics	Brief description
GFA	the gross floor area of all the built space
FAR	GFA divided by the parcel area
SCR	area of the ground floor building footprints divided by the area of the site
DEG	the rate at which density falls, based on the distance from the location of reference (Section, Figure 2)
HLB	height of the lowest building on the edge of the district (Section, Figure 2)
CES	cell, defined by a block and its adjacent street; the size of a cell is consist of the size of the block contained and a half of the adjacent street width (Plan, Figure 2)
LUR	ratio of the built areas of residential (RES), commerical (COM), and office (OFF) land use
BFO	angle of the building's main façade's orientation, zero degrees from the South (Plan, Figure 2)
DBB	distance between buildings in adjacent cells (Plan, Figure 2)

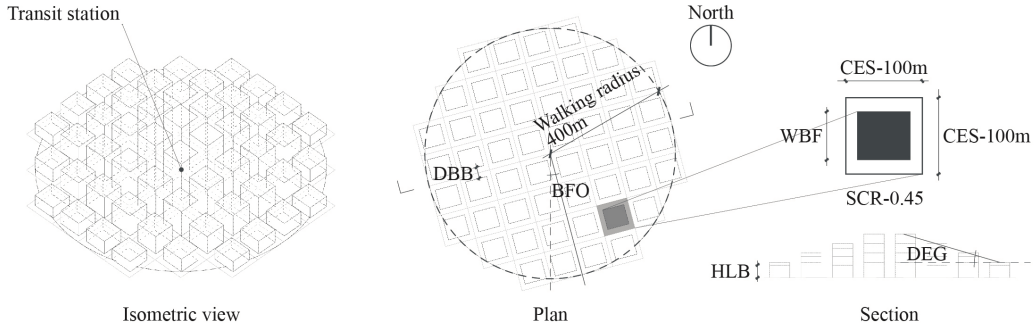

Figure 2. The parametric model of urban form generation

10 meters' increment), BFO (0-180 degrees, with 10 degrees' increment), and the share of residential (RES), commercial (COM), and office (OFF) land use. As SCR was set as a parameter and the building footprint is a rectangle, DBB became a dependent variable of WBF. We set up six scenarios for different density gradients, namely with a DEG at 0°, 5°, 10°, 15°, 20°, and 25°. The DEG could not exceed 25°, as a higher DEG would result in a FAR that exceeds the norm ($3.0 \leq FAR \leq 25.0$) of high-density cells in the Singapore Master Plan (Urban Redevelopment Authority, 2016). The respective hourly energy demand profiles for weekdays and weekends in Singapore are depicted in Figure 3. In Singapore, it was assumed that the space cooling load and the domestic hot water heating load was identical throughout the year. We assumed that vapor compression chillers running with electricity satisfy all cooling loads. Therefore, all of the demand in the district was supplied with electricity.

To assess the energy generation capacity of the district under different urban scenarios, we set up a simulation model in EnergyPlus for PV electricity generation. The electricity generated from PV was simulated in EnergyPlus over the period of the most typical week near the annual average (30 July to 5 August) at hourly time-step. The typical week was retrieved from the EnergyPlus Weather File (EPW) of Singapore (EnergyPlus, 2017). It was assumed that 100% of the building rooftops and building facades were covered with PV panels. The inputs to the simulation model were building geometry and the incident solar radiation data from the EPW. The incident solar radiation on PV panel surfaces was calculated based on the building surface geometry, accounting for shading with other buildings. With the incident radiation on the PV panel surfaces, the electricity production was predicted with a quasi-steady state equivalent one-diode model (Griffith and Ellis, 2004).

We adopted Octopus present in Grasshopper as the multi-objective optimization engine for this study. Based on the experiences from previous research (Hsieh et al., 2017),

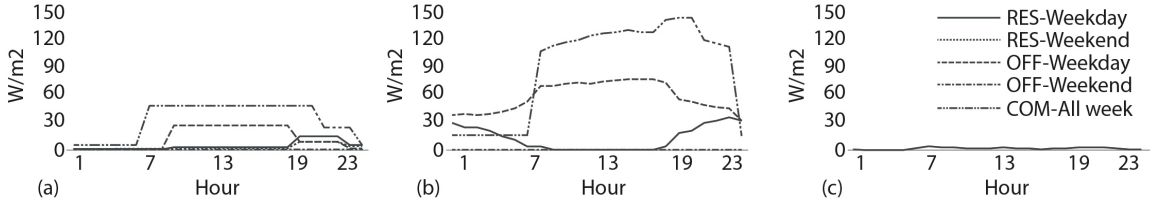

Figure 3. Daily profiles of (a) electricity consumption for appliances and lighting (b) cooling load (c) domestic hot water (DHW) load depending on day types and land use (Hsieh et al., 2017).

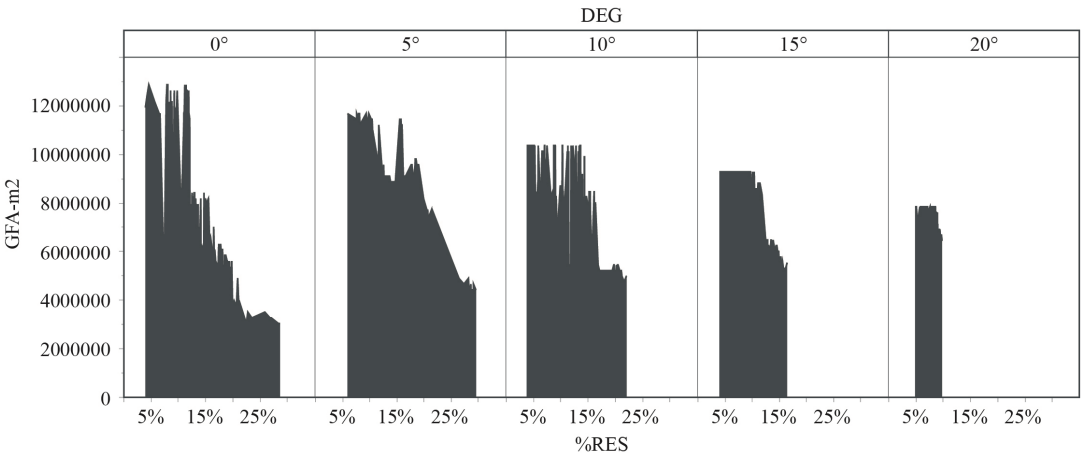

Figure 4. The range of GFA, %RES achieved in dependence on DEG.

three objectives were chosen. The first was to maximize the share of renewable energy (%RES). The second was to maximize the GFA, as following the first objective only would result in reducing the GFA down to the minimum. The third was to minimize the grid connection capacity, namely the peak electricity imported from the grid (PDG). In each scenario, the decision variables were HLB, BFO, WBF, RES, COM, and OFF. SCR and DEG were constant in this formulation. The FAR of each cell was constrained between 3 and 25. The optimization was run for 20 individuals and 20 generations to limit the computational expense.

The resulting Pareto-front was obtained by performing non-dominated sorting of the entire population obtained from optimization. In a multi-objective optimization problem, an individual solution 'A' was deemed to be non-dominated, when there was no other individual with all objectives better than 'A'. In this work, %RES (maximize), GFA (maximize) and PDG (minimize) were the objectives. The Pareto-front presented did not have a solution which had higher %RES, higher GFA, and lower PDG compared to any other presented solutions.

Results (ZS/SH, 500)

We used JMP 13 (SAS Institue Inc., 2016) to process the data acquired through the six scenarios with a DEG of 0°, 5°, 10°, 15°, 20°, and 25°, and generated the figures in this section. In the sixth scenario with a DEG of 25°, all the valid solutions have the same GFA, due to the FAR constraints of each cell, thus omitting one optimization objective. Therefore, we excluded it from the result comparison and discussion as follows.

Figure 4 shows the trends of the maximum GFA and the range of %RES reachable in the five scenarios with various DEGs. Within each scenario, it can be observed that there is a trend that the maximum GFA decreases as the %RES mounts after a certain point. For example, when DEG is of 0°, as %RES mounts to the peak, GFA drops 76.3% compared to its peak. Such an interrelation justifies our assumption

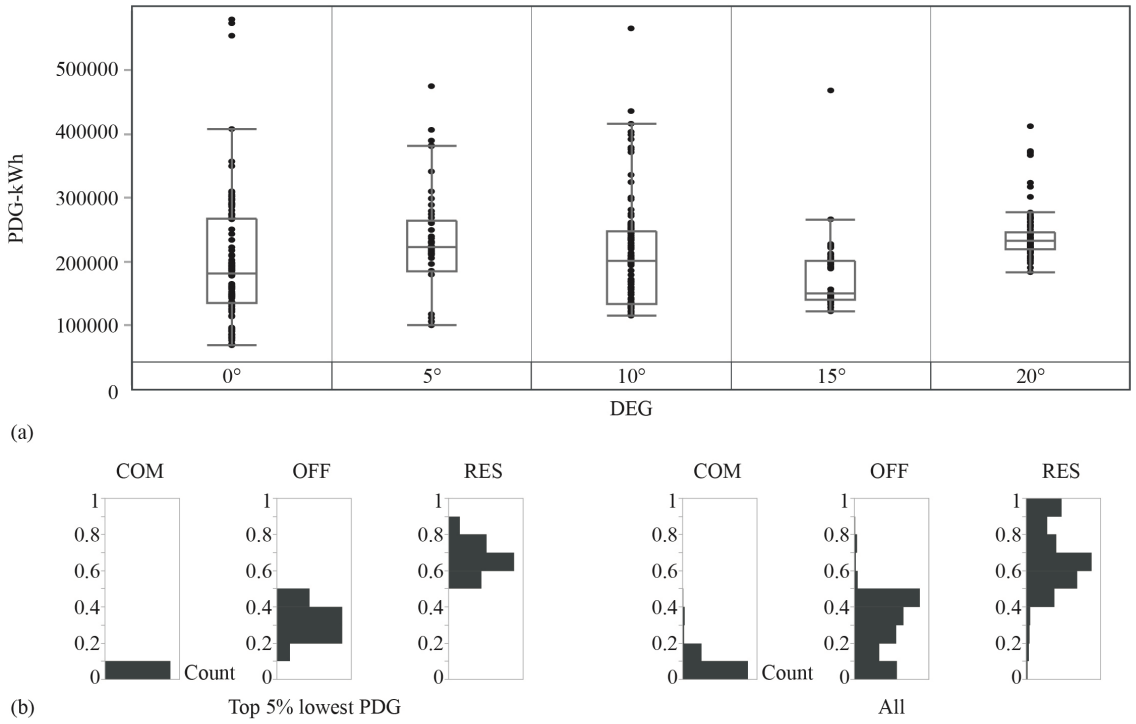

Figure 5. (a) range of PDG achieved in dependence on DEG (b) distributions of the three land use of all individuals and those ranking the lowest 5% by PDG.

about the interrelation between the first two optimization objectives in the optimization setup. However, before reaching the critical point, as the %RES mounts, the GFA remains constant until a certain point before it starts to decrease. These points are critical for the tradeoff between the GFA and the % RES. At these points, the share of RES is increased to above 95%, while COM and OFF are both reduced to the least.

Across all five scenarios, the %RES achieved spreads in a range from 3.7 – 29.6%. The maximum achievable % RES reaches the highest with a DEG of 5° and drops drastically as the DEG increases. The %RES can reach above 20% only in the scenarios with a DEG at 0°, 5° and 10°. For a DEG of 0°, the range is the largest (4 – 28.6%), for 5°, the range is the second largest (5.9-29.6%). The ranges are rather large as, besides DEG, HLB also has a relatively substantial influence on the %RES, as it can strongly affect the achievable GFA. %RES decreases drastically as GFA increases, in general.

There are 583 individuals in total, across the five Pareto-fronts (DEG = 0°, 5°, 10°, 15°, and 20°). We sorted them based on their PDG. Figure 5a shows the range of PDG achieved with respect to DEG. The lowest PDG is with a DEG of 0°. The lowest PDG achieved in each scenario tends to increase with a higher PDG. Figure 5b shows the combinations of land use, including RES, COM, and OFF, of all individuals and those, whose PDG ranks in the top 5% smallest, respectively. All the individuals that fall into the top 5% have a DEG of 0°. Compared to all, the three land uses tend of the top 5% have narrower spectrum, with a RES of 54-80% and a OFF of 20-45%. COM tends to approach to 0-3%. As COM

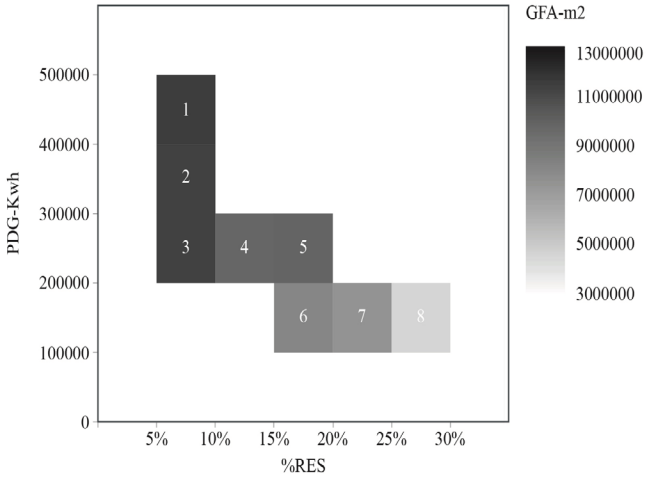

Figure 6. Eight groups of the individuals on the Pareto-front with a DEG of 5°.

Table 2. The representative individuals behind each of the eight groups.

Group	Design variables						Objectives		
	COM	OFF	RES	HLB (m)	BFO (°)	WBF (m)	%RES	GFA (m^2)	PDG (MWh)
1	0%	78%	22%	141	70	70	7.6%	11682000	407
2	0%	74%	26%	141	0	70	7.9%	11682000	390
3	2%	38%	60%	141	0	70	9.8%	11682000	280
4	1%	35%	64%	108	0	80	12.4%	9108000	212
5	0%	1%	99%	117	170	70	18.5%	9810000	237
6	0%	4%	96%	96	0	80	19.9%	8172000	197
7	0%	1%	99%	90	0	80	21.4%	7704000	186
8	0%	4%	96%	48	0	80	29.6%	4428000	106

has a higher energy intensity, the optimization reduced COM to increase the %RES.

We took the scenario with a DEG of 5°, which has the comparatively largest range of achievable GFA, PDG, and %RES, into further discussion and comparison. Figure 6 divides the individuals on the Pareto-front into eight groups based on the three objectives. Table 2 compares the design variables of the representative individual behind each of the eight groups. Group 2 and 3 have similar %RES and GFA, as well as the same HLB, BFO, and WBF. The different distributions of the land use caused the huge difference on PDG. Group 4 and 5 have similar PDG and GFA, as well as similar HLB, BFO, and WBF. The sharp differences between the share of OFF and RES use lead to the differences in %RES.

Conclusions

Through this pilot study, we adopted the method of simulation-based urban form generation and optimization to study the mechanism of how urban form, regarding density and land use, affects the share of renewable energy (%RES) and peak electricity import from the grid (PDG). We took six design variables into consideration, including HLB, BFO, WBF, RES, COM, and OFF for six scenarios with different DEG. The three-optimization objectives we set are: maximizing %RES, maximizing GFA, and minimizing PDG.

For each of the five scenarios with a DEG equals to 0°, 5°, 10°, 15°, and 20°, respectively, we observed a break point until which GFA remains at the peak as %RES mounts. From that point onwards, a significant increase of %RES may cause a sacrifice up to as much as 76.3% of GFA. Maintaining the same GFA, in order to peak %RES, the results tend to maximize RES to above 95% and minimize the other uses, since the residential land use has the lowest total demand. In transit-oriented districts in Singapore, the highest %RES achievable is 30% with a DEG 5°. %RES can reach above 20% with a DEG under 10°. The distributions of land use have substantial influences on both %RES and PDG. Due to its high energy demand, commercial land use has negative impacts on the achievable %RES. To achieve a higher %RES, the urban planners may consider reducing the commercial uses within a reasonable range. The specific results and their interpretation are location specific and need to be viewed in the context of the site and its climate. The general mechanisms observed, however also apply to other locations.

The study presented in this work has certain limitations. First, it used a transit-oriented district typology (a pyramid shape). Other district typologies exist, for example of stair shape and corona shape (Kämpf and Robinson, 2010). The stair shape represents a typology with a magnificent view on one side. The corona shape represents a typical district typology with a plaza or lower buildings surrounded by taller buildings. According to the research of Kämpf and Robinson, the corona shape yields a high solar potential.

Second, there are limitations with regards to the street patterns. Though the grid pattern is common in new projects, many other street patterns exist as well. Similarly, we adopt the podium building pattern in this research, while other building patterns should also be considered. For example, a court building pattern provides more façade and less rooftop area for PV panel installations. Furthermore, we used density and land use as relevant metrics in the early stage of an urban project, however, other metrics may also have a substantial influence on the performance of PV panels. For example, the window-to-wall ratio will impact the space for PV panel installations on the facades. The building envelope material with different albedos will also influence the solar radiation captured by the PV panels. Finally, there are limitations regarding the calculation of energy demand. As mutual shading will affect the electricity generation by the PV panels, it may also decrease the cooling demand and thus affect the %RES. However, in this work, when calculating the energy demand of the buildings, we did not take the influence of mutual shading into consideration.

The study of the interdependencies between urban form and various energy technologies is crucial for establishing the concept of energy-driven urban design (Shi et al., 2017). It aims to increase urban energy performance through

maximizing the performance of the energy technologies in conjunction with urban form.

References

Arbour & Associés (2001) Faubourg Québec, paramètres de développement urbain (Société de développement de Montréal, Montréal).

Cervero, R., Guerra, E., 2011. Urban densities and transit: a multi-dimensional perspective. UC Berkeley Center for Future Urban Transport, Berkeley.

EnergyPlus, 2017. Singapore 486980 (IWEC) [WWW Document]. URL https://www.energyplus.net/weather-download/southwest_pacific_wmo_region_5/SGP//SGP_Singapore.486980_IWEC/all (accessed 6.20.17).

EnergyPlus Energy Simulation Software, 2017. . DOE, Golden, USA.

Griffith, B.T., Ellis, P.G., 2004. Photovoltaic and Solar Thermal Modeling with the EnergyPlus Calculation Engine: Preprint. Presented at the World Renewable Energy Congress VIII and Expo, Denver, Colorado.

Hsieh, S., Schüler, N., Shi, Z., Fonseca, J.A., Maréchal, F., Schlueter, A., 2017. Defining density and land uses under energy performance targets at the early stage of urban planning processes, in: CISBAT 2017 International Conference - Future Buildings & Districts - Urban Form, Energy and Technology. Presented at the CISBAT 2017, Lausanne, Switzerland.

IEA ECBCS Annex51 - Subtask B, 2012. Case studies on energy planning and implementation strategies for neighborhoods, quarters and municipal areas.

Kämpf, J.H., Robinson, D., 2010. Optimisation of building form for solar energy utilisation using constrained evolutionary algorithms. Energy Build. 42, 807–814. doi:10.1016/j.enbuild.2009.11.019

Luther, J., Reindl, T., 2014. Solar Photovoltaic (PV) Roadmap for Singapore (A Summary). Solar Energy Research Institute of Singapore (SERIS), Singapore.

Olszewski, P., Wibowo, S., 2005. Using Equivalent Walking Distance to Assess Pedestrian Accessibility to Transit Stations in Singapore. Transp. Res. Rec. J. Transp. Res. Board 1927, 38–45. doi:10.3141/1927-05

Sanaieian, H., Tenpierik, M., Linden, K. van den, Mehdizadeh Seraj, F., Mofidi Shemrani, S.M., 2014. Review of the impact of urban block form on thermal performance, solar access and ventilation. Renew. Sustain. Energy Rev. 38, 551–560. doi:10.1016/j.rser.2014.06.007

SAS Institue Inc., 2016. JMP 13. Cary, NC.

Seto, K.C., Güneralp, B., Hutyra, L.R., 2012. Global forecasts of urban expansion to 2030 and direct impacts on biodiversity and carbon pools. Proc. Natl. Acad. Sci. U. S. A. 109, 16083–16088.

Shi, Z., Fonseca, J.A., Schlueter, A., 2017. A review of simulation-based urban form generation and optimization for energy-driven urban design. Build. Environ. 121, 119–129. doi:10.1016/j.buildenv.2017.05.006

UN-Habitat, 2012. Energy [WWW Document]. URL http://unhabitat.org/urban-themes/energy/ (accessed 11.8.16).

Urban Redevelopment Authority, 2017. Development control parameters for non-residential development. Singapore.

Urban Redevelopment Authority, 2016. Master Plan [WWW Document]. URL https://www.ura.gov.sg/uol/master-plan.aspx?p1=view-master-plan# (accessed 2.16.17).